Rates of magma transfer in the crust: Insights into magma reservoir recharge and pluton growth

Thierry Menand, Catherine Annen, Michel de Saint Blanquat

Publisher: GSA
Journal: GEOL: Geology
DOI:10.1130/G36224.1

Rates of magma transfer in the crust: Insights into magma reservoir recharge and pluton growth

Thierry Menand[1], Catherine Annen[2], and Michel de Saint Blanquat[3]

[1]*Laboratoire Magmas et Volcans, Université Blaise Pascal - CNRS - IRD, OPGC, 5 rue Kessler, 63038 Clermont-Ferrand, France*

[2]*School of Earth Sciences, University of Bristol, Wills Memorial Building, Bristol BS8 1RJ, UK*

[3]*Geosciences Environnement Toulouse, Université de Toulouse, CNRS, IRD, OMP, 14 avenue Edouard-Belin, 31400 Toulouse, France*

ABSTRACT

Plutons have long been viewed as crystallized remnants of large magma reservoirs, a concept now challenged by high precision geochronological data coupled with thermal models. Similarly, the classical view of silicic eruptions fed by long-lived magma reservoirs that slowly differentiate between mafic recharges is being questioned by petrological and geophysical studies. In both cases, a key and yet unresolved issue is the rate of magma transfer in the crust. Here, we use thermal analysis of magma transport to calculate the minimum rate of magma transfer through dykes. We find that unless the crust is exceptionally hot the recharge of magma reservoirs requires a magma supply rate of at least ~0.01 km^3/yr, much higher than the long-term growth rate of plutons, which demonstrates unequivocally that igneous bodies must grow incrementally. This analysis argues also that magma reservoirs are short-lived and erupt rapidly after being recharged by already differentiated magma. These findings have significant implications for the monitoring of dormant volcanic systems and our ability to interpret geodetic surface signals related to incipient eruptions.

Publisher: GSA
Journal: GEOL: Geology
DOI:10.1130/G36224.1

INTRODUCTION

Petrological and geophysical studies challenge the long-held view that silicic magma reservoirs are long-lived, differentiating slowly between mafic recharges. For example, until recently Santorini volcano, Greece, was understood as a volcano whose shallow dacitic reservoir is regularly recharged by small mafic spurts (Martin et al., 2008). However, crystal diffusion chronometry and surface deformation data reveal a different story. In the case of the ~1600 BC Minoan caldera-forming eruption, reactivation was fast (< 100 years) with a transient recharge flux > 0.05 km^3/yr, more than 50 times the long-term magma influx that feeds the volcano (Druitt et al., 2012). Crucially, reactivation represented a sizable proportion of the shallow reservoir, and involved an already differentiated magma of deep origin (Druitt et al., 2012). Similar conclusions are reached for Santorini's recent activity (Parks et al., 2012). The emerging view is thus of a volcano whose shallow reservoir is regularly replenished from depth by high-flux batches of already differentiated magma, the duration of which is much shorter than that of intervening repose periods. These findings raise key but unresolved questions: what determine the recharge rate of shallow reservoirs? And ultimately, can we identify recharges that will lead to an eruption? These are crucial issues in volcanology, and not simply at Santorini.

These issues also echo that of the rates at which pluton assembly occurs (Petford et al., 2000; Cruden and McCaffrey, 2001; Glazner et al., 2004; Saint Blanquat et al., 2011). Indeed, the example of Santorini fits with models for the generation of evolved magmas in deep crustal hot zones (Annen et al., 2006) and the incremental emplacement and growth of igneous bodies in the upper crust (Menand et al., 2011). According to the deep hot zone model (Annen et al., 2006), the chemical diversity of arc magmas and granites is generated in the lower crust. After leaving their deep hot zones, the vast majority of magmas stall below the surface, many of them

Publisher: GSA
Journal: GEOL: Geology
DOI:10.1130/G36224.1

as sills and often amalgamating together to form larger plutons as evidenced by geological, geophysical and geochronological data (e.g., Hawkes and Hawkes, 1933; Cruden, 1998; Benn et al., 1999; Saint Blanquat et al., 2001; Al-Kindi et al., 2003; Cruden, 2006; Michel et al., 2008; Horsman et al., 2009; Leuthold et al., 2012). It is in the upper crust that magmas acquire their textural diversity owing to shallow-level crystallization. Incremental growth of plutons is widely accepted, and the issue is now to identify the incremental processes involved and to quantify their rates. The recharge of volcano reservoirs and the growth of plutons seem intimately related: in both cases, the key point is the rate of magma transfer between a source and a shallower storage level.

THERMAL ANALYSIS

Magma transport in the crust occurs mainly through dykes (Lister and Kerr, 1991; Clemens and Mawer, 1992; Petford et al., 1993) but there is currently no 3D, time-dependent propagation model. We therefore focused our analysis on the steady-state propagation of buoyant dykes, and performed a stochastic thermal analysis to quantify the minimum volumetric flow rates that are required for dykes to transport magma through Earth's crust.

Dykes need to propagate fast enough through the crust to avoid death by solidification (Spence and Turcotte, 1985; Rubin 1995). Flowing magma advects heat along dykes while heat is conducted away by the colder country rocks. If advection is slower than conduction then the magma will solidify and dyke propagation will cease. A buoyant dyke intruding rocks of fracture toughness K_c over some height H must thus be fed with a critical minimum magma supply rate (details in Supplemental information[1])

$$Q_c = \frac{9}{32}\left[\frac{C_p\left(T_f - T_\infty\right)^2}{L\left(T_0 - T_f\right)}\right]^{9/4}\left(\frac{\Delta\rho g \kappa^3 H^3}{\mu}\right)^{1/4}\left(\frac{K_c}{\Delta\rho g}\right)^{2/3}, \quad (1)$$

Publisher: GSA
Journal: GEOL: Geology
DOI:10.1130/G36224.1

where L is magma latent heat, C_p is its specific heat capacity, T_o, T_f and T_∞ are initial magma, freezing and crustal far-field temperatures, respectively, μ is magma dynamic viscosity, κ is its thermal diffusivity, $\Delta\rho$ is the density difference between country rocks and magma, and g is gravitational acceleration. This is the minimum influx of magma a buoyant dyke needs to propagate over a height H without freezing. A growing pluton would need to be fed with at least this influx of magma Q_c, which would thus represent a short-term magma supply rate, otherwise its feeder dyke would freeze before it could reach this emplacement level. The same goes for the recharge of an existing reservoir lying a height H above a deeper magma source; Q_c would then represent a short-term magma recharge or replenishment rate.

RESULTS

We used Monte Carlo simulations to calculate the expected range of critical rates for magmas with viscosities between 10 and 10^8 Pa s. Magmatic and country-rock parameters were sampled randomly, and three different ranges of far-field temperatures T_∞ were tested: cold, intermediate or hot crusts (Table 1). In each case T_∞ was kept constant throughout the crust, a simplification (no geothermal gradient) that may underestimate magma heat lost hence Q_c.

Figure 1A shows the range of critical short-term supply rates Q_c as a function of magma viscosity from 10 000 Monte Carlo simulations for a 5-km-high dyke in a crust with intermediate far-field temperature ($T_\infty = 200 - 400$ °C). For all magma viscosities, the simulations give a range of critical rates Q_c with a normal distribution around a mean value on a logarithmic scale (Fig. 1B). This allows a minimum supply rate $Q_{c\min}$ to be defined, three standard deviations

Publisher: GSA
Journal: GEOL: Geology
DOI:10.1130/G36224.1

below the mean value; statistically, more than 99% of the calculated rates lie above $Q_{c\min}$ (Fig. 1).

Figure 2 shows this minimum supply rate $Q_{c\min}$ as a function of magma viscosity for two dyke heights, 5 km and 30 km, and various far-field temperatures. $Q_{c\min}$ decreases with increasing magma viscosity: fluid dynamics dictate that more viscous magmas induce thicker dykes, and because thicker dykes cool more slowly the net effect is a lower minimum supply rate (details in Supplemental information[1]). Hotter crusts lead to lower amounts of heat loss hence lower minimum supply rates; this nonlinear effect can reduce $Q_{c\min}$ by several orders of magnitude. Longer propagation heights require higher supply rates $Q_{c\min}$. For the most conservative scenario of dykes propagating over 5 km in a hot crust ($T_\infty = 400 - 600$ °C), a minimum supply rate of 10^{-4} to 4×10^{-3} km^3/yr is required to transport magmas with viscosities between 10 and 10^8 Pa s (Fig. 2). Longer magma-transport heights and colder environments (T_∞ < 200 °C) lead to higher minimum supply rates (> 0.01 km^3/yr).

Figure 3 compares the density distribution of all the critical short-term supply rates Q_c calculated by Monte Carlo simulations with the density distribution of 47 published maximum, long-term-averaged, pluton-filling-rate estimates (Table DR1, Supplemental information[1]). There is a clear dichotomy between pluton-filling rates and our critical short-term supply rates, which has several important implications. First, irrespective of pluton emplacement depth, magma composition and tectonic setting, nearly all the reported plutons have too low a magma supply rate to have formed by a single episode of magma injection. This means that the formation of these plutons must have involved successive, discrete magma pulses with a short-term injection rate for their successive feeder dykes of at least ~0.01 km^3/yr (Fig. 3). We note that some of the

Publisher: GSA
Journal: GEOL: Geology
DOI:10.1130/G36224.1

few reported filling-rate estimates greater than 0.01 km^3/yr exhibit strong evidence for incremental growth (e.g., Papoose Flat pluton; Saint Blanquat et al., 2001) or are associated with particularly hot crusts (e.g., Japan; Tanaka, 2002; Socorro Magma body, Reiter et al., 2010), in agreement with our findings that hotter crusts allow magma transport in dykes at much lower flow rates (Fig. 2). Moreover, most of the larger estimated filling rates are derived from observations of surface deformation integrated over at most two decades; they should be close to short-term supply rates and are indeed in agreement with our minimum fluxes. Second, $Q_{c\min}$ should also be the absolute minimum short-term recharge rate of magma reservoirs, such as that of Santorini volcano. A value of ~0.01 km^3/yr is in agreement with the recharge rates estimated for the Minoan eruption or the current activity at Nea Kameni (Druitt et al., 2012; Parks et al., 2012), as well as the latest estimates for the recent magma supply or recharge rates at Lazufre volcanic complex in the Central Andes (Remy et al., 2014). Estimates determined for timescales of one to several decades (Lazufre, Santorini) probably integrate repose periods. Discrete recharge rates are likely to be larger (Usu-san, Syowa Sinzan). Finally, filling rates based on deformation are typically one order of magnitude larger than those based on geochronology (Table DR1, Supplemental information[1]), suggesting intermittent feeding over various time-scales.

IMPLICATIONS

According to our thermal analysis, the feeding of volcanoes by magmas from depth requires a short-term supply rate greater than ~0.01 km^3/yr. However, a storage region can only develop into a potentially active reservoir with a sizeable amount of eruptible magma if the time-averaged supply rate exceeds 0.001 – 0.01 km^3/yr (Annen, 2009). For lower time-averaged supply rates, the volume of eruptible magma available at anyone time is at best that of a single

Publisher: GSA
Journal: GEOL: Geology
DOI:10.1130/G36224.1

magmatic recharge event. Since most igneous bodies are emplaced at low time-averaged rates (Fig. 3), large eruptions require that either the repose time between recharges becomes transiently shorter, leading to a sharp increase in magma influx (Schöpa and Annen, 2013), or a recharge is exceptionally prolonged and rapidly brings in a large volume of magma that is erupted shortly after the intrusive event.

Evidence for rapid short-term recharge rates is not restricted to Santorini volcano. According to element diffusion models, the 530 km^3 of silicic magma erupted during the Oruanui eruption had been assembled within ~1600 years, implying an average flux of at least 0.3 km^3/yr, and most of the erupted volume was injected ~200 years before the eruption (Allan et al., 2013). Similarly, quartz crystallization times in the Bishop tuff magma are estimated to have occurred within 500–3000 years before eruption (Gualda et al., 2012). From these data and our analysis we suggest that long-lived magma bodies in the middle or deep crust feed ephemeral shallow reservoirs that erupt shortly after their formation over a few centuries or millennia. Because there are long periods of no or low activity between such magmatic high-flux feeding episodes, the long-term construction rate of plutons assembled from intrusions that failed to feed a shallower reservoir or to erupt is much lower than the reservoir assembly rate recorded by erupted crystals. This sporadic assembly must occur at several levels in the lower and upper crust; from mass balance, since only part of the magma stored in a reservoir continues toward the surface, we expect long-term fluxes to decrease for successively shallower reservoirs. Magma reservoirs can be long-lived in the deep crust because of higher ambient temperature, whereas in the cold shallow crust, magmas that do not erupt shortly after emplacement solidify rapidly. Moreover, magmas emplaced at high rates relatively close to the surface may induce such high

Publisher: GSA
Journal: GEOL: Geology
DOI:10.1130/G36224.1

stresses in the cold, brittle crust that eruption is almost unavoidable (Jellinek and DePaolo, 2003).

Our analysis raises the question of our ability to interpret geodetic surface signals: differentiating between surface deformation produced by an new influx of magma bound to form a frozen pluton from one associated with a reservoir recharge, when both scenarios require the same minimum short-term magma influx. Which parameters do we need to determine in order to make such a distinction? Our analysis implies that one cannot tell from a single magma pulse what will happen next: a pulse must have a minimum short-term flux in order to be thermally viable whatever the thermal fate of the storage region it might be feeding (pluton or volcanic reservoir). However, a key point is that the fate of this storage region hinges upon its time-averaged supply rate, integrated over several magma pulses (Annen, 2009; Schöpa and Annen, 2013). Diffusion chronometry provides access to timescales that are commensurate with the fast emplacement rates of magma intrusions but requires material that has already been erupted. Continuous geodetic measurements of volcano surface deformation (e.g., Remy et al., 2014) could provide a means to estimate recharge volumes and rates integrated over several magma pulses, and thus the potential to discriminate between magmatic intrusions bound to crystallize, owing to a too slow time-averaged supply rate, from those recharging a reservoir at fast enough rates to potentially lead to future eruptions.

ACKNOWLEDGMENTS

We thank A.R. Cruden, Allen Glazner and an anonymous reviewer for their thorough and critical reviews. We acknowledge supports from a chaire mixte IRD-UBP, ERC Advanced Grants "CRITMAG" and "VOLDIES", and the CNRS-INSU programme Syster. This research was partially funded by the French Government Laboratory of Excellence initiative n°ANR-10-

Publisher: GSA
Journal: GEOL: Geology
DOI:10.1130/G36224.1
LABX-0006, the Région Auvergne and the European Regional Development Fund. This is Laboratory of Excellence ClerVolc contribution number 130.

REFERENCES CITED

Al-Kindi, S., White, N., Sinha, M., England, R., and Tiley, R., 2003, Crustal trace of a hot convective sheet: Geology, v. 31, p. 207–210, doi:10.1130/0091-7613(2003)031<0207:CTOAHC>2.0.CO;2.

Allan, A.S.R., Morgan, D.J., Wilson, C.J.N., and Millet, M.-A., 2013, From mush to eruption in centuries: Assembly of the super-sized Oruanui magma body: Contributions to Mineralogy and Petrology, v. 166, p. 143–164, doi:10.1007/s00410-013-0869-2.

Annen, C., 2009, From plutons to magma chambers: Thermal constraints on the accumulation of eruptible silicic magma in the upper crust: Earth and Planetary Science Letters, v. 284, p. 409–416, doi:10.1016/j.epsl.2009.05.006.

Annen, C., Blundy, J.D., and Sparks, R.S.J., 2006, The genesis of intermediate and silicic magmas in deep crustal hot zones: Journal of Petrology, v. 47, p. 505–539, doi:10.1093/petrology/egi084.

Atkinson, B.K., 1984, Subcritical crack growth in geological materials: Journal of Geophysical Research, v. 89, p. 4077–4114, doi:10.1029/JB089iB06p04077.

Benn, K., Roest, W.R., Rochette, P., Evans, N.G., and Pignotta, G.S., 1999, Geophysical and structural signatures of syntectonic batholith construction: The South Mountain Batholith, Meguma Terrane, Nova Scotia: Geophysical Journal International, v. 136, p. 144–158, doi:10.1046/j.1365-246X.1999.00700.x.

Bohrson, W.A., and Spera, F.J., 2001, Energy-constrained open-system magmatic processes II: Application of energy-constrained assimilation-fractional crystallization (EC-AFC) model to

Publisher: GSA
Journal: GEOL: Geology
DOI:10.1130/G36224.1
magmatic systems: Journal of Petrology, v. 42, p. 1019–1041, doi:10.1093/petrology/42.5.1019.

Clemens, J.D., and Mawer, C.K., 1992, Granitic magma transport by fracture propagation: Tectonophysics, v. 204, no. 3–4, p. 339–360, doi:10.1016/0040-1951(92)90316-X.

Cruden, A.R., 1998, On the emplacement of tabular granites *in* Clemens, J.D., ed.: Journal of the Geological Society of London, Special Issue on Granitoid Magma Dynamics, v. 155, p. 853–862.

Cruden, A.R., 2006, Emplacement and growth of plutons: Implications for rates of melting and mass transfer in continental crust, *in* Brown, M., and Rushmer, T., eds., Evolution and Differentiation of the Continental Crust: New-York, Cambridge University Press, p. 455–519.

Cruden, A.R., and McCaffrey, K.F.W., 2001, Growth of plutons by floor subsidence: Implications for rates of emplacement, intrusion spacing and melt-extraction mechanisms: Physics and Chemistry of the Earth, v. 26, p. 303–315, doi:10.1016/S1464-1895(01)00060-6.

Delaney, P.T., and Pollard, D.D., 1981, Deformation of host rocks and flow of magma during growth of minette dikes and breccia-bearing intrusions near Ship Rock, New Mexico: U.S. Geological Survey Professional Paper 1202, 61 p.

Druitt, T.H., Costa, F., Deloule, E., Dungan, M., and Scaillet, B., 2012, Decadal to monthly timescales of magma transfer and reservoir growth at a caldera volcano: Nature, v. 482, p. 77–80, doi:10.1038/nature10706.

Glazner, A.F., Bartley, J.M., Coleman, D.S., Gray, W., and Taylor, R.Z., 2004, Are plutons assembled over millions of years by amalgamation from small magma chambers?: GSA Today, v. 14, p. 4–11, doi:10.1130/1052-5173(2004)014<0004:APAOMO>2.0.CO;2.

Gualda, G.A.R., Pamukcu, A.S., Ghiorso, M.S., Anderson, A.T., Jr., Sutton, S.R., and Rivers, M.L., 2012, Timescales of quartz crystallization and the longevity of the Bishop giant magma body: PLoS ONE, v. 7, p. e37492, doi:10.1371/journal.pone.0037492.

Hawkes, L., and Hawkes, H.K., 1933, The Sandfell Laccolith and 'Dome of Elevation': Quarterly Journal of the Geological Society, v. 89, p. 379–400, doi:10.1144/GSL.JGS.1933.089.01-04.14.

Heimpel, M., and Olson, P., 1994, Buoyancy-driven fracture and magma transport through the lithosphere: Models and experiments *in* Ryan, M.P., ed., Magmatic Systems: San Diego, Academic Press, p. 223–240.

Horsman, E., Morgan, S., Saint Blanquat, M. de, Habert, G., Nugnet, A., Hunter, R.A., and Tikoff, B., 2009, Emplacement and assembly of shallow intrusions from multiple magma pulses, Henry Mountains, Utah: Earth and Environmental Science Transactions of the Royal Society of Edinburgh, v. 100, p. 117–132, doi:10.1017/S1755691009016089.

Jellinek, A.M., and DePaolo, D.J., 2003, A model for the origin of large silicic magma chambers: precursors of caldera-forming eruptions: Bulletin of Volcanology, v. 65, p. 363–381, doi:10.1007/s00445-003-0277-y.

Kojitani, H., and Akaogi, M., 1994, Calorimetric study of olivine solid solutions in the system Mg2SiO4-Fe2SiO4: Physics and Chemistry of Minerals, v. 20, p. 536–540, doi:10.1007/BF00211849.

Lange, R.A., Cashman, K.V., and Navrotsky, A., 1994, Direct measurements of latent heat during crystallization and melting of a ugandite and an olivine basalt: Contributions to Mineralogy and Petrology, v. 118, p. 169–181, doi:10.1007/BF01052867.

Leuthold, J., Müntener, O., Baumgartner, L.P., Putlitz, B., Ovtcharova, M., and Schaltegger, U., 2012, Time resolved construction of a bimodal laccolith (Torres del Paine, Patagonia): Earth and Planetary Science Letters, v. 325–326, p. 85–92, doi:10.1016/j.epsl.2012.01.032.

Lister, J.R., and Kerr, R.C., 1991, Fluid-mechanical models of crack propagation and their application to magma transport in dykes: Journal of Geophysical Research, v. 96, B6, p. 10,049–10,077, doi:10.1029/91JB00600.

Martin, V.M., Morgan, D.J., Jerram, D.A., Caddick, M.J., Prior, D.J., and Davidson, J.P., 2008, Bang! Month-scale eruption triggering at Santorini volcano: Science, v. 321, p. 1178, doi:10.1126/science.1159584.

Menand, T., Annen, C., and Saint Blanquat, M. de, 2011, Emplacement of magma pulses and growth of magma bodies: Tectonophysics, v. 500, p. 1–2, doi:10.1016/j.tecto.2010.05.014.

Michel, J., Baumgartner, L., Putlitz, B., Schaltegger, U., and Ovtcharova, M., 2008, Incremental growth of the Patagonian Torres del Paine laccolith over 90 ky: Geology, v. 36, p. 459–462, doi:10.1130/G24546A.1.

Mysen, B.O., 1981, Melting curves of rocks and viscosity of rock-forming melts, *in* Touloukian, Y.S., Judd, W.D., and Roy, R.F., eds., Physical Properties of rocks and minerals, Data series on material properties 2: New York, McGraw -Hill/CINDAS, p. 361–407.

Parks, M.M., Biggs, J., England, P., Mather, T.A., Nomikou, P., Palamartchouk, K., Papanikolaou, X., Paradissis, D., Parsons, B., Pyle, D.M., Raptakis, C., and Zacharis, V.,

Publisher: GSA
Journal: GEOL: Geology
DOI:10.1130/G36224.1
2012, Evolution of Santorini volcano dominated by episodic and rapid fluxes of melt from depth: Nature Geoscience, v. 5, p. 749–754, doi:10.1038/ngeo1562.

Petford, N., Kerr, R.C., and Lister, J.R., 1993, Dike transport in granitoid magmas: Geology, v. 21, p. 845–848, doi:10.1130/0091-7613(1993)021<0845:DTOGM>2.3.CO;2.

Petford, N., Cruden, A.R., McCaffrey, K.J.W., and Vigneresse, J.-L., 2000, Granite magma formation, transport and emplacement in the Earth's crust: Nature, v. 408, p. 669–673, doi:10.1038/35047000.

Piwinskii, A.J., and Wyllie, P.J., 1968, Experimental studies of igneous rock series: A zoned pluton in the Wallowa Batholith, Oregon: The Journal of Geology, v. 76, p. 205–234, doi:10.1086/627323.

Reiter, M., Chamberlin, R.M., and Love, D.W., 2010, New data reflect on the thermal antiquity of the Socorro magma body locale, Rio Grande Rift, New Mexico: Lithosphere, v. 2, p. 447–453.

Remy, D., Froger, J.L., Perfettini, H., Bonvalot, S., Gabalda, G., Albino, F., Cayol, V., Legrand, D., and Saint Blanquat, M. de, 2014, Persistent uplift of the Lazufre volcanic complex (Central Andes): New insights from PCAIM inversion of InSAR time series and GPS data: Geochemistry Geophysics Geosystems, doi:10.1002/2014GC005370.

Robertson, E.C., 1988, Thermal Properties of Rocks: U.S. Geological Survey Open-file Report 88-441, p. 1–110.

Rubin, A.M., 1995, Getting granite dikes out of the source region: Journal of Geophysical Research, v. 100, p. 5911–5929.

Saint Blanquat, M. de, Law, R.D., Bouchez, J.-L., and Morgan, S.S., 2001, Internal structure and emplacement of the Papoose Flat pluton: An integrated structural, petrographic, and

magnetic susceptibility study: Geological Society of America Bulletin, v. 113, p. 976–995, doi:10.1130/0016-7606(2001)113<0976:ISAEOT>2.0.CO;2.

Saint Blanquat, M. de, Horsman, E., Habert, G., Morgan, S., Vanderhaeghe, O., Law, R., and Tikoff, B., 2011, Multiscale magmatic cyclicity, duration of pluton construction, and the paradoxical relationship between tectonism and plutonism in continental arcs: Tectonophysics, v. 500, p. 20–33.

Schöpa, A., and Annen, C., 2013, The effects of magma flux variations on the formation and lifetime of large silicic magma chambers: Journal of Geophysical Research, v. 118, p. 926–942.

Spence, D.A., and Turcotte, D.L., 1985, Magma-driven propagation of cracks: Journal of Geophysical Research, v. 90, p. 575–580.

Spera, F.J., 2000, Physical properties of magmas, *in* Sigurdsson, H., Houghton, B., Rymer, H., Stix, J., and McNutt, S., eds., Encyclopedia of Volcanoes: San Diego, Academic Press, p. 171–190.

Tanaka, A., and Ishikawa, Y., 2002, Temperature distribution and focal depth in the crust of the northeastern Japan: Earth Planets Space, v. 54, p. 1109–1113.

Wagner, T.P., Donnelly-Nolan, J.M., and Grove, T.L., 1995, Evidence of hydrous differentiation and crystal accumulation in the low-MgO, high-Al2O3 Lake Basalt from Medicine Lake volcano, California: Contributions to Mineralogy and Petrology, v. 121, p. 201–216, doi:10.1007/s004100050099.

Whittington, A.G., Hofmeister, A.M., and Nabelek, P.I., 2009, Temperature-dependent thermal diffusivity of the Earth's crust and implications for magmatism: Nature, v. 458, p. 319–321, doi:10.1038/nature07818.

Publisher: GSA
Journal: GEOL: Geology
DOI:10.1130/G36224.1

FIGURE CAPTIONS

Figure 1. Critical magma supply rates Q_c from 10 000 Monte Carlo simulations for a 5-km-high buoyant dyke in intermediate crust ($T_\infty = 200 - 400$ °C). A, Range of Q_c as a function of magma viscosity. The continuous black curve is the mean Q_c. The dashed black curve is the minimum critical supply rate $Q_{c\min}$ defined as the mean Q_c minus three standard deviations. B, Histogram of the Monte Carlo simulations for a magma viscosity of 10^4 Pa s. On a logarithmic scale, this histogram is well fitted by a normal distribution with a mean of 2.32 and a standard deviation of 1.04, hence $Q_{c\min}$ ~0.16 km^3/yr.

Figure 2. Minimum magma influx $Q_{c\min}$ to prevent magma freeze. Two vertical propagation distances are considered (5 km, continuous line; 30 km, dashed line) as a function of magma viscosity and far-field temperature (squares: $T_\infty = 50 - 200$ °C; triangles: $T_\infty = 200 - 400$ °C; circles: $T_\infty = 400 - 600$ °C).

Figure 3. Probability density estimates (normal kernel function) of 47 maximum, long-term-averaged pluton-filling rates (dashed curve, Table DR1, Supplemental information[1]) and of 10 000 Monte-Carlo critical supply rates Q_c (continuous curve, parameters ranges in Table 1, far-field temperatures sampled according to sampled dyke heights (between 5 and 30 km): $T_\infty = 400 - 600$ °C for heights > 20 km, $T_\infty = 200 - 600$ °C for heights > 10 km, $T_\infty = 50 - 600$ °C for shorter dykes).

[1]GSA Data Repository item 2015xxx, Supplemental information, is available online at www.geosociety.org/pubs/ft2015.htm, or on request from editing@geosociety.org or Documents Secretary, GSA, P.O. Box 9140, Boulder, CO 80301, USA.

Figure 1
Click here to download high resolution image

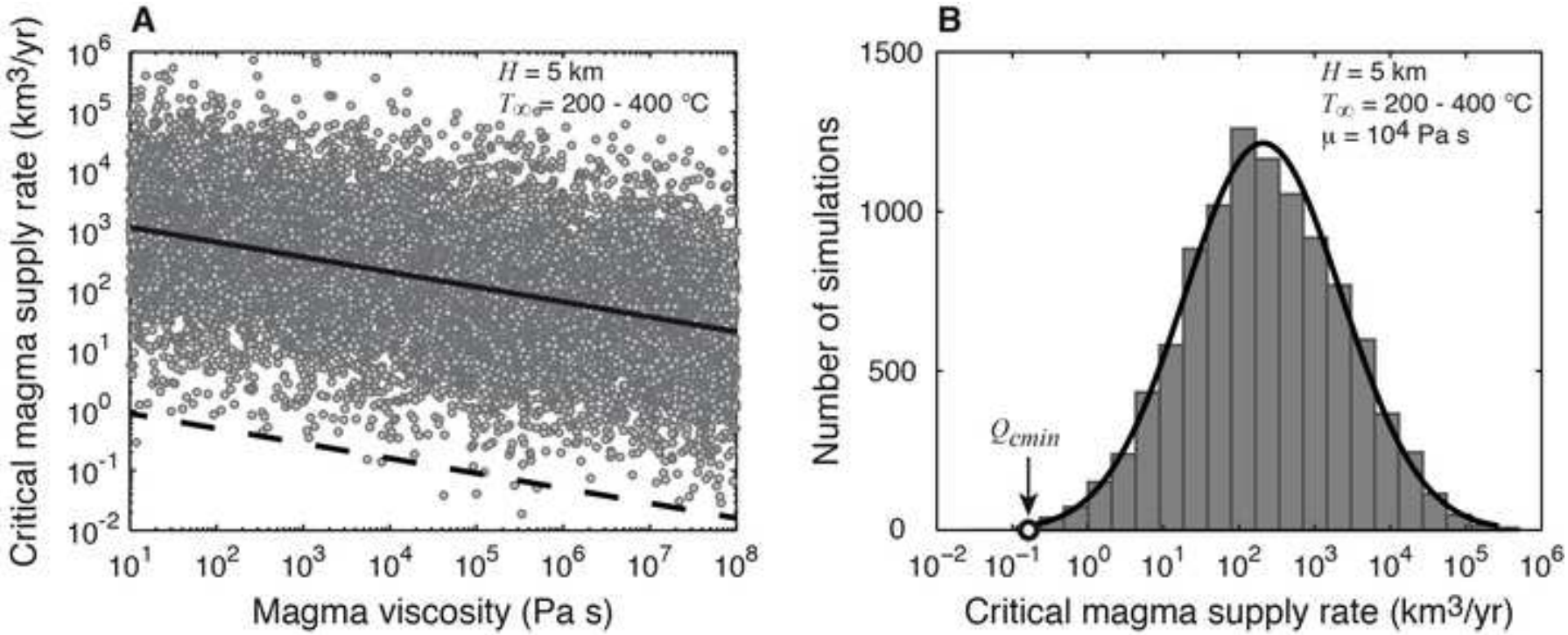

Figure 2
Click here to download high resolution image

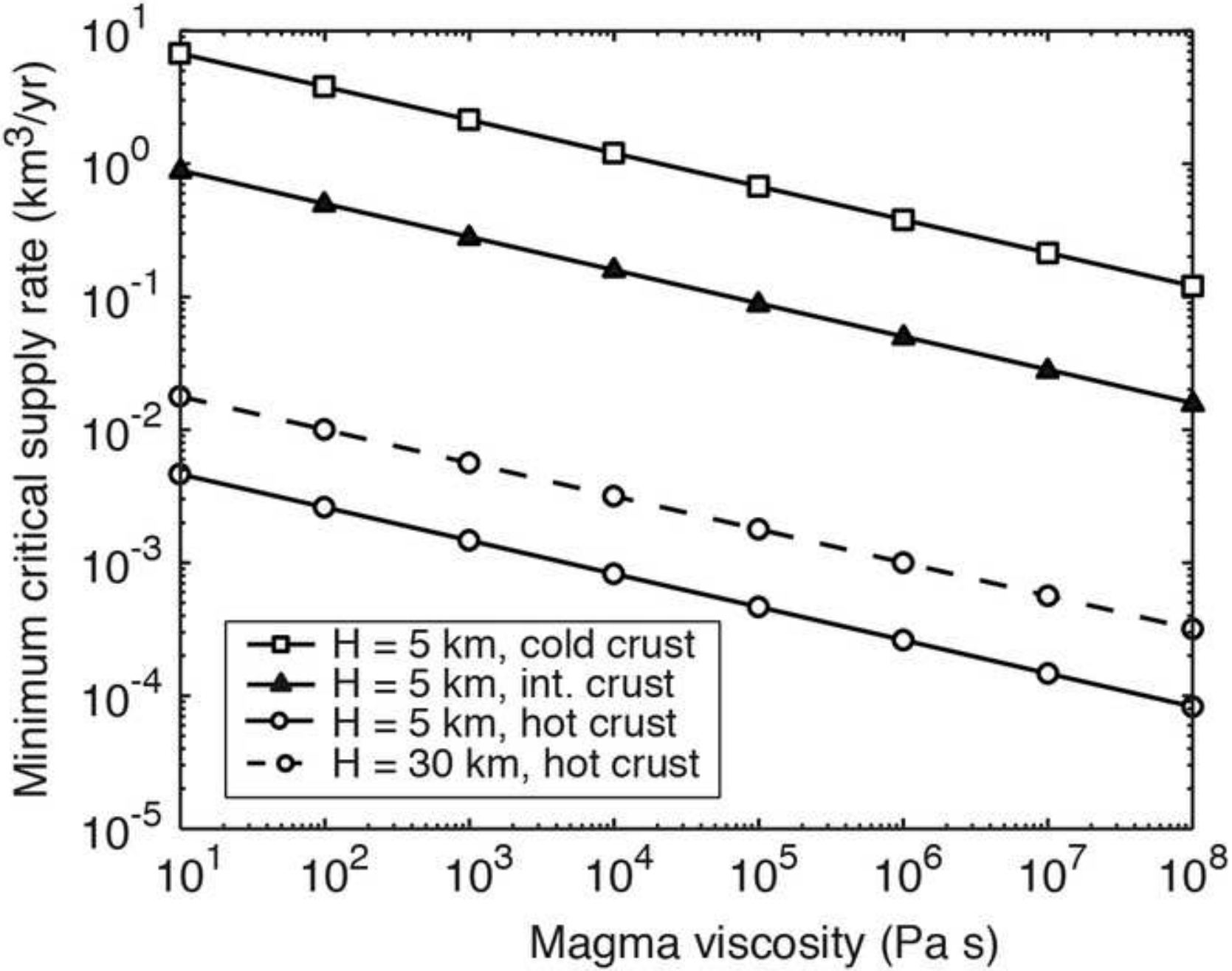

Figure 3
Click here to download high resolution image

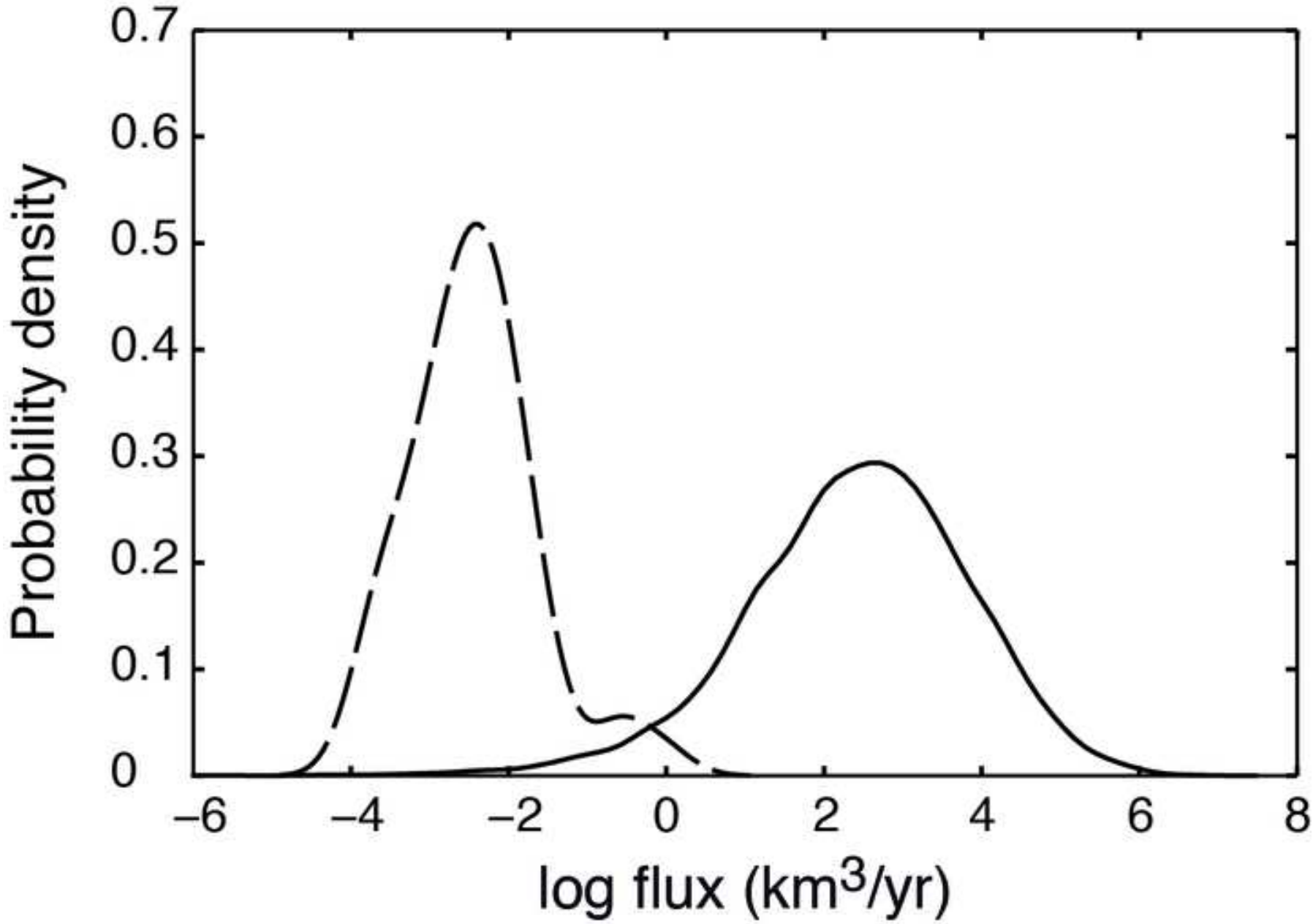

Table 1

TABLE 1. PARAMETER RANGES AND DISTRIBUTIONS USED IN MONTE CARLO SIMULATIONS.

Parameter	Distribution	Min	Max	Mean
Magma viscosity (Pa s)	uniform	10	10^8	-
Latent heat L (J/kg)[a-c]	uniform	2.5×10^5	5.5×10^5	-
Specific heat C_p (J/kg K)[a,d]	uniform	800	1600	-
Thermal diffusivity κ (m^2/s)[e]	uniform	0.3×10^{-6}	2.0×10^{-6}	-
Fracture toughness K_c (Pa $m^{1/2}$)[f-h]	log-normal	10^6	10^9	$10^{7.5}$
Density contrast $\Delta\rho$ (kg/m^3)[i]	uniform	100	700	-
Magma temperature T_o (^oC)[j]	uniform	750	1250	-
Freezing temperature $T_f = T_o - \Delta T_i$: ΔT_i (^oC)[k,l]	uniform	20	200	-
Far field temperature T_∞ (^oC):				
Cold crust	uniform	50	200	-
Int. crust	uniform	200	400	-
Hot crust	uniform	400	600	-

Note: The (Max - Min) range of the $\log(K_c)$ normal distribution was equated with six standard deviations. a: Bohrson and Spera (2001); b: Kojitani and Akaogi (1994); c : Lange et al. (1994); d: Robertson (1988); e: Whittington et al. (2009); f: Atkinson (1984); g: Delaney and Pollard (1981); h: Heimpel and Olson (1994; i: Spera (2000); j: Mysen (1981); k: Piwinskii and Wyllie (1968); l: Wagner et al. (1995).

GSA Supplemental information

Supplemental information for: Rates of magma transfer in the crust: insights into magma reservoir recharge and pluton growth by Thierry Menand, Catherine Annen, and Michel de Saint Blanquat.

STEADY-STATE PROPAGATION OF A BUOYANCY-DRIVEN DYKE

Whether fed by a constant flux or a constant pressure from its source, a vertically propagating buoyant dyke will ultimately reach the same steady state once its vertical extent becomes greater than its buoyancy length $L_b = \left(\frac{K_c}{\Delta\rho g} \right)^{2/3}$ (Lister and Kerr, 1991; Menand and Tait, 2002), where K_c is the fracture toughness of the country rocks, $\Delta\rho$ is the density difference between country rocks and magma, and g is the gravitational acceleration. This steady state is characterised by a constant vertical velocity and a constant volumetric flow rate (Lister and Kerr, 1991; Menand and Tait, 2002). Importantly, the steady-state dyke geometry is also characterised by a constant thickness w away from its propagating upper tip, at a distance greater than $\sim 4L_b$ (Lister, 1990), determined by the constant incoming flux of magma delivered by its feeding source. For the vast majority of dykes, magma flow is laminar and the steady-state dyke thickness depends on the magma viscosity μ, the density difference between country rocks and magma $\Delta\rho$, the gravitational acceleration g, the dyke horizontal extent B and the average volumetric magma flow rate Q as $w = \left(\frac{12\mu Q}{\Delta\rho g B} \right)^{1/3}$ (Lister and Kerr, 1991). The average

volumetric magma flow rate can thus be expressed as a function of the other parameters:

$$Q = \frac{\Delta\rho g w^3 B}{12\mu}. \quad \text{(DR1)}$$

Another characteristic feature of a steadily propagating buoyant dyke is that its horizontal dimension B is approximately constant and equal to the buoyancy length of the dyke (Menand and Tait, 2001; 2002): $B \approx \left(\frac{K_c}{\Delta\rho g} \right)^{2/3}$. There is presumably a constant of proportionality between the horizontal dimension B and the buoyancy length L_b depending on the exact shape of the dyke, but this shape factor will most likely remain of order one. Moreover, the variability in horizontal dimension will be most affected by the range of possible values in both the rock fracture toughness K_c and the density difference $\Delta\rho$ between magma and country rocks. [In the case the host rock has a negligible fracture toughness, the horizontal dimension of a buoyant dyke will instead increase with the distance z above its source as $z^{3/10}$, however for the range of fracture-toughness values considered in Table 1 this horizontal spread of the dyke will be prevented (Lister and Kerr, 1991).]

10 000 Monte-Carlo simulations with values for K_c and $\Delta\rho$ sampled randomly within the ranges of values listed in Table 1 give an overall range of horizontal dimensions B between 400 m and 200 km with 80% of the B values smaller than 20 km, a mean value of ~13 km and a mode value of ~5 km (Fig. DR1). These calculated values are in excellent agreement with observed dyke dimensions, and thus suggest the scaling law used for B captures the appropriate range of geological dimensions. The average volumetric magma flow rate in a vertically propagating steady-state buoyant dyke can thus be expressed as

$$Q = \frac{\Delta\rho g w^3}{12\mu}\left(\frac{K_c}{\Delta\rho g}\right)^{2/3}. \quad \text{(DR2)}$$

CRITICAL MINIMUM MAGMA FLOW RATE

In order to be able to propagate over some distance *H*, a dyke must have a critical minimum thickness w_c so that magma may ascend through the crust over this distance without freezing (Petford et al., 1993):

$$w_c = 1.5\left[\frac{C_p\left(T_f - T_\infty\right)^2}{L\left(T_0 - T_f\right)}\right]^{3/4}\left(\frac{\mu\kappa H}{\Delta\rho g}\right)^{1/4}. \quad \text{(DR3)}$$

L is magma latent heat, C_p is its specific heat capacity, T_o, T_f and T_∞ are the initial magma, freezing and crustal far-field temperatures, respectively, μ is magma dynamic viscosity, κ is its thermal diffusivity, $\Delta\rho$ is the density difference between country rocks and magma, and *g* is gravitational acceleration. Dykes that are thinner than this critical thickness freeze before they could propagate as far as the distance *H* whereas thicker dykes could propagate even further, and even possibly melt some of the country rocks (Bruce and Huppert, 1989).

Although Equation (DR3) gives the minimum thickness a dyke must have to be thermally able to transport magma over some distance in the crust, this equation does not provide any constraint on the dyke dynamics. Indeed, dykes of the same thickness could a priori involve different magma fluxes, hence different amounts of advected heat. Considering magma flow as laminar and buoyancy-driven within a dyke of thickness w and intruding rocks of fracture toughness K_c, the magma average volumetric flow rate is given by Equation (DR2),

$Q = \frac{\Delta\rho g w^3}{12\mu}\left(\frac{K_c}{\Delta\rho g}\right)^{2/3}$. Combining this expression with Equation (DR3) yields the magma volumetric flow rate in a dyke with the critical thickness w_c:

$$Q_c = \frac{9}{32}\left[\frac{C_p\left(T_f - T_\infty\right)^2}{L\left(T_0 - T_f\right)}\right]^{9/4}\left(\frac{\Delta\rho g \kappa^3 H^3}{\mu}\right)^{1/4}\left(\frac{K_c}{\Delta\rho g}\right)^{2/3}. \quad \text{(DR4)}$$

This critical magma supply rate Q_c is the volumetric flow rate that allows a dyke to propagate over a distance H without freezing.

A counterintuitive result is that this critical, minimum flux decreases with magma viscosity: more viscous dykes can flow at lower fluxes and not freeze. The key point here is that both the volumetric flux in a dyke, Q, and the critical dyke thickness, w_c, depend on the magma viscosity but the flux itself does depend also on the thickness: the flux in a buoyant dyke is proportional to the third power of the dyke thickness and inversely proportional to the magma viscosity, $Q \propto w^3\mu^{-1}$, (Equation DR2). We are dealing with the minimum volumetric flux that would allow a buoyant dyke to propagate over a given distance, and so this flux must be associated with the critical thickness of that dyke, $Q_c \propto w_c^3\mu^{-1}$. Because the critical thickness varies as the magma viscosity to the 1/4th power (Equation DR3), $w_c \propto \mu^{1/4}$, the combine effect of this dependency with that of the flux leads to the minimum flux as decreasing with the magma viscosity to the 1/4th power, $Q_c \propto \mu^{-1/4}$. In other words, fluid dynamics dictate that more viscous magmas induce thicker dykes (Equation DR2), and because thicker dykes cool more slowly the net effect is a lower minimum supply rate (Equation DR4). We note, however, that this dependency results in a minimal effect of magma viscosity on the critical, minimum flux Q_c: an

78 increase of viscosity by eight orders of magnitude will reduce the minimum flux by only a factor
79 100.

80 **PARAMETER RANGES AND DISTRIBUTIONS IN MONTE CARLO SIMULATIONS**

81 The ranges of parameters used in the Monte Carlo simulations were taken from the
82 following references: Latent heat L from Bohrson and Spera (2001), Kojitani and Akaogi (1994),
83 and Lange et al. (1994); specific heat C_p from Bohrson and Spera (2001) and Robertson (1988);
84 thermal diffusivity κ from Whittington et al. (2009); fracture toughness K_c from Atkinson
85 (1984), Delaney and Pollard (1981), and Heimpel and Olson (1994); density contrast $\Delta\rho$ from
86 Spera (2000); initial magma temperature T_o from Mysen (1981); difference between the initial
87 and freezing magma temperatures ΔT_i from Piwinskii and Wyllie (1968), and Wagner et al.
88 (1995).

89 For each parameter, there was not enough data to enable us to favour one particular
90 distribution relative to others. A uniform distribution was therefore chosen as it gives the same
91 weight to all data. The only exception is the rock fracture toughness K_c. There is a long debate as
92 to its true representative values, with measurements from laboratory-scale rock samples giving
93 values of about 10^6 Pa $m^{1/2}$ (Atkinson; 1984) while field-scale fracture toughness values can be
94 up to 3 orders of magnitude greater (Delaney and Pollard, 1981; Heimpel and Olson, 1994).
95 Instead of arbitrarily favouring one set of values more than the other, we chose to sample the
96 whole range with a log-normal distribution. This corresponded to sampling the exponent values
97 between 6 and 9 with a normal distribution around a mean value of 7.5 that is comparable with
98 both laboratory- and field-derived values. Furthermore, a log-normal distribution diminishes the
99 weight attributed to extreme values, whether laboratory- or field-based, and leads to a range of

values for the dyke breadth B in very good agreement with field observations as shown in Fig. DR1.

FIGURE CAPTIONS

Figure DR1. Probability density estimate (normal kernel function) of 10 000 Monte-Carlo horizontal steady-state dimensions B for a buoyancy-driven dyke (parameter ranges in Table 1).

106 **TABLE DR1. ESTIMATES OF MAXIMUM, LONG-TERM AVERAGED, PLUTON-**

107 **FILING RATES.**

System	Max. long-term filling rate (km^3/yr)	Method
Boulder batholith[a]	6.3×10^{-3}	Isotope
New Guinea Highlands[a]	4.7×10^{-3}	isotope
Guichon Creek batholith, B.C.[a]	2.1×10^{-4}	isotope
Sierra Nevada batholith[a]	8.3×10^{-4}	isotope
Sierra Nevada batholith[a]	6.9×10^{-4}	isotope
Sierra Nevada batholith[a]	1.9×10^{-3}	isotope
Sierra Nevada batholith[a]	6.8×10^{-3}	isotope
Sierra Nevada batholith[a]	1.9×10^{-3}	isotope
Southern California batholith[a]	6.9×10^{-3}	isotope
Alaska-Aleutian Range batholith[a]	9.8×10^{-3}	isotope
New England batholith, Australia[a]	2.3×10^{-3}	isotope
Lachlan batholithic belt, Australia[a]	3.1×10^{-3}	isotope
Peruvian Coastal batholith[a]	1.2×10^{-2}	isotope
Coast Range Plutonic Complex, B.C.[a]	1.4×10^{-2}	isotope
Black Mesa[b]	5.0×10^{-3}	thermal
Papoose Flat[c]	2.5×10^{-2}	thermal
Tuolumne[d]	1.2×10^{-3}	isotope
Scuzzy[e]	3.0×10^{-3}	isotope
Socorro[f]	2.8×10^{-1}	thermal

Hualca Hualca[g]	2.5×10^{-2}	deformation
Uturuncu[g]	3.0×10^{-2}	deformation
Lazufre[g]	6.0×10^{-3}	deformation
Mt Stuart Batholith[h]	2.2×10^{-4}	isotope
Mt Stuart Batholith old domain[h]	5.8×10^{-4}	isotope
Mt Stuart Batholith young domain[h]	3.1×10^{-3}	isotope
Tenpeak intrusion[h]	1.5×10^{-4}	isotope
Geyser-Cobb Mountain[i]	1.5×10^{-3}	isotope
Wiborg batholith[j]	3.6×10^{-3}	isotope
Wiborg batholith[j]	6.0×10^{-3}	isotope
Nain plutonic suite[k]	4.8×10^{-3}	isotope
Nain plutonic suite[k]	2.2×10^{-3}	isotope
Korosten complex[l]	4.0×10^{-3}	isotope
Korosten complex[l]	1.2×10^{-2}	isotope
Salmi complex[m]	9.3×10^{-3}	isotope
Salmi complex[m]	2.4×10^{-3}	isotope
Lastarria Cordon del Azufre[n,u]	1.4×10^{-2}	deformation
Torres del Paine (granite)[o]	8.0×10^{-4}	isotope
Torres del Paine (mafic)[o]	2.0×10^{-4}	isotope
Manaslu[p]	6.0×10^{-4}	thermal
PX1, Fuerteventura[q]	3.0×10^{-4}	thermal
Uturuncu[r]	1.0×10^{-2}	deformation
Spirit Mountain batholith[s,t]	1.3×10^{-3}	isotope

Usu-san[v]	9.2×10^{-1}	deformation
Syowa Sinzan[w]	2.1×10^{-1}	deformation
Lamark Granodiorite[x]	2.0×10^{-3}	isotope
John Muir Intrusive Suite[x]	1.0×10^{-3}	isotope
Rio Hondo[y]	2.7×10^{-4}	isotope

These long-term-averaged pluton-filling-rate estimates assume no loss of material over time from the plutons, and reflect also the assumptions made by the various authors about their actual size and shape. a: Crisp (1984); b: Saint Blanquat et al. (2006); c: Saint Blanquat et al. (2001); d: Coleman et al. (2004); e: Brown and McClelland (2000); f: Pearse and Fialko (2010); g: Prittchard and Simmons (2002); h: Matzel et al. (2006); i: Schmitt et al. (2003); j: Vaasjoki et al. (1991); k: Emslie et al. (1994); l: Amelin et al. (1994); m: Amelin et al. (1997); n: Froger et al. (2007); o: Leuthold et al. (2012); p: Annen et al. (2006); q: Allibon et al. (2011); r: Sparks et al. (2008), s: Walker et al. (2007); t: Miller et al. (2011); u: Remy et al. (2014); v: Omori (1911); w: Minakami et al. (1951); x: Davis et al. (2012); y: Tappa et al. (2011).

REFERENCES

Allibon, J., Bussy, F., Léwin, E., and Darbellay, B., 2011, The tectonically controlled emplacement of a vertically sheeted gabbro-pyroxenite intrusion: Feeder-zone of an ocean-island volcano (Fuerteventura, Canary Islands): Tectonophysics, v. 500, p. 78–97.

Amelin, Y.V., Heaman, L.M., Verchogliad, V.M., and Skobelev, V.M., 1994, Geochronological constraints on the emplacement history of an anorthosite-rapakivi granite suite: U-Pb zircon and baddeleyite study of the Korosten complex, Ukraine: Contrib. Mineral. Petrol., v. 116, p. 411–419.

126 Amelin, Y.V., Larin, A.M., and Tucker, R.D., 1997, Chronology of multiphase emplacement of
127 the Salmi rapakivi granite-anorthosite complex, Baltic Shield: implications for magmatic
128 evolution: Contrib. Mineral. Petrol., v. 127, p. 353–368.
129 Annen, C., Scaillet, B., and Sparks, R.S.J., 2006, Thermal constraints on the emplacement rate of
130 a large intrusive complex: the Manaslu leucogranite, Nepal Himalaya: J. Petrol., v. 47, p.
131 71–95.
132 Atkinson, B.K., 1984, Subcritical crack growth in geological materials: Journal of Geophysical
133 Research, v. 89, p. 4077–4114, doi:10.1029/JB089iB06p04077.
134 Bohrson, W.A., and Spera, F.J., 2001, Energy-constrained open-system magmatic processes II:
135 Application of energy-constrained assimilation-fractional crystallization (EC-AFC) model to
136 magmatic systems: Journal of Petrology, v. 42, p. 1019–1041,
137 doi:10.1093/petrology/42.5.1019.
138 Brown, E.H., and McClelland, W.C., 2000, Pluton emplacement by sheeting and vertical
139 ballooning in part of the southeast Coast Plutonic Complex, British Columbia: Geol. Soc.
140 Am. Bull., v. 112, p. 708–719.
141 Bruce, P.M., and Huppert, H.H., 1989, Thermal control of basaltic eruptions: Nature, v. 342, p.
142 665–667.
143 Coleman, D.S., Gray, W., and Glazner, A.F., 2004, Rethinking the emplacement and evolution
144 of zoned plutons: Geochronologic evidence for incremental assembly of the Tuolumne
145 Intrusive Suite, California: Geology, v. 32, p. 433–436.
146 Crisp, J.A., 1984, Rates of magma emplacement and volcanic output: J. Volcanol. Geotherm.
147 Res., v. 20, p. 177–211.

148 Davis, J.W., Coleman, D.S., Gracely, J.T., Gaschnig, R., and Stearns, M., 2012, Magma
149 accumulation rates and thermal histories of plutons of the Sierra Nevada batholith, CA:
150 Contrib. Mineral. Petrol., v. 163, p. 449–465.
151 Delaney, P.T., and Pollard, D.D., 1981, Deformation of host rocks and flow of magma during
152 growth of minette dikes and breccia-bearing intrusions near Ship Rock, New Mexico: U.S.
153 Geological Survey Professional Paper 1202, 61 p.
154 Emslie, R.F., Hamilton, M.A., and Thériault, R.J., 1994, Petrogenesis of a Mid-Proterozoic
155 Anorthosite-Mangerite-Charnockite-Granite (AMCG) complex: isotopic and chemical
156 evidence from the Nain plutonic suite: J. Geol., v. 102, p. 539–558.
157 Froger, J.L., Remy, D., Bonvalot, S., and Legrand, D., 2007, Two scales of inflation at Lastarria-
158 Cordon del Azufre volcanic complex, central Andes, revealed from ASAR-ENVISAT
159 interferometric data: Earth Planet. Sci. Lett., v. 255, p. 148–163.
160 Heimpel, M., and Olson, P., 1994, Buoyancy-driven fracture and magma transport through the
161 lithosphere: Models and experiments in Ryan, M.P., ed., Magmatic Systems: San Diego,
162 Academic Press, p. 223–240.
163 Kojitani, H., and Akaogi, M., 1994, Calorimetric study of olivine solid solutions in the system
164 Mg2SiO4-Fe2SiO4: Physics and Chemistry of Minerals, v. 20, p. 536–540,
165 doi:10.1007/BF00211849.
166 Lange, R.A., Cashman, K.V., and Navrotsky, A., 1994, Direct measurements of latent heat
167 during crystallization and melting of a ugandite and an olivine basalt: Contributions to
168 Mineralogy and Petrology, v. 118, p. 169–181, doi:10.1007/BF01052867.

169 Leuthold, J., Müntener, O., Baumgartner, L. P., Putlitz, B., Ovtcharova, M., and Schaltegger, U.,
170 2012, Time resolved construction of a bimodal laccolith (Torres del Paine, Patagonia): Earth
171 Planet. Sci. Lett., v. 325-326, p. 85–92.
172 Lister, J.R., 1990, Buoyancy-driven fluid fracture: the effects of material toughness and of low-
173 viscosity precursors: J. Fluid Mech., v. 210, 263-280.
174 Lister, J.R., and Kerr, R.C., 1991, Fluid-mechanical models of crack propagation and their
175 application to magma transport in dykes: J. Geophys. Res., v. 96(B6), p. 10,049-10,077.
176 Matzel, J.E.P., Bowring, S.A., and Miller, R.B., 2006, Time scales of pluton construction at
177 differing crustal levels: Examples from the Mount Stuart and Tenpeak intrusions, North
178 Cascades, Washington: Geol. Soc. Am. Bull., v. 118, p. 1412–1430.
179 Menand, T., and Tait, S.R., 2001, A phenomenological model for precursor volcanic eruptions:
180 Nature, v. 411, p. 678-680.
181 Menand, T., and Tait, S.R., 2002, The propagation of a buoyant liquid-filled fissure from a
182 source under constant pressure: An experimental approach: J. Geophys. Res., v. 107(B11),
183 2306, doi:10.1029/2001JB000589.
184 Minakami, T., Ishikawa, T., and Yagi, K., 1951, The 1944 eruption of volcano Usu in Hokkaido,
185 Japan: Volcanological Bulletin, v. 11, p. 45–157.
186 Miller, C.F., Furbish, D. J., Walker, B. A., Claiborne, L. L., Koteas, G. C., Bleick, H. A., and
187 Miller, J. S., 2011, Growth of plutons by incremental emplacement of sheets in crystal-rich
188 host: Evidence from Miocene intrusions of the Colorado River region, Nevada, USA:
189 Tectonophysics, v. 500, p. 65–77.

Mysen, B.O., 1981, Melting curves of rocks and viscosity of rock-forming melts, in Touloukian, Y.S., Judd, W.D., and Roy, R.F., eds., Physical Properties of rocks and minerals, Data series on material properties 2: New York, McGraw -Hill/CINDAS, p. 361–407.

Omori, F., 1911, The Usu-San eruption and earthquakes and elevation phenomena: Bulletin of the Imperial Earthquake Investigation Committee, v. 5, p. 1–38.

Pearse, J., and Fialko, Y., 2010, Mechanics of active magmatic intraplating in the Rio Grande Rift near Socorro, New Mexico: J. Geophys. Res., v. 115, B07413.

Piwinskii, A.J., and Wyllie, P.J., 1968, Experimental studies of igneous rock series: A zoned pluton in the Wallowa Batholith, Oregon: The Journal of Geology, v. 76, p. 205–234, doi:10.1086/627323.

Prittchard, M.E., and Simmons, M., 2002, A satellite geodetic survey of large- scale deformation of volcanic centres in the central Andes: Nature, v. 418, p. 1–5.

Remy, D., Froger, J.L., Perfettini, H., Bonvalot, S., Gabalda, G., Albino, F., Cayol, V., Legrand, D., and Saint Blanquat (de), M., 2014, Persistent uplift of the Lazufre volcanic complex (Central Andes): new insights from PCAIM inversion of InSAR time series and GPS data: Geochem. Geophys. Geosyst., doi: 10.1002/2014GC005370.

Robertson, E.C., 1988, Thermal Properties of Rocks: U.S. Geological Survey Open-file Report 88-441, p. 1–110.

Saint Blanquat (de), M., Habert, G., Horsman, E., Morgan, S.S., Tikoff, B., Laneau, P., and Gleizes, G., 2006, Mechanisms and duration of non-tectonically assisted magma emplacement in the upper crust: The Black Mesa pluton, Henry Mountains, Utah: Tectonophysics, v. 428, p. 1–31.

212 Saint Blanquat (de), M., Law, R.D., Bouchez, J.-L., and Morgan, S.S., 2001, Internal structure
213 and emplacement of the Papoose Flat pluton: An integrated structural, petrographic, and
214 magnetic susceptibility study: Geol. Soc. Am. Bull., v. 113, p. 976–995.
215 Schmitt, A.K., Grove, M., Harrison, T. M., Lovera, O., Hulen, J., and Walters, M., 2003, The
216 Geysers-Cobb Mountain Magma System, California (Part 2): timescales of pluton
217 emplacement and implications for its thermal history: Geochim. Cosmochim. Acta, v. 67, p.
218 3443–3458.
219 Sparks, R.S.J., Folkes, C., Humphreys, M., Barfod, D., Clavero, J., Sunagua, M., McNutt, S., and
220 Pritchard, M., 2008, Uturuncu volcano, Bolivia: Volcanic unrest due to mid-crustal magma
221 intrusion: Am. J. Sci., v. 308, p. 727–769.
222 Spera, F.J., 2000, Physical properties of magmas, in Sigurdsson, H., Houghton, B., Rymer, H.,
223 Stix, J., and McNutt, S., eds., Encyclopedia of Volcanoes: San Diego, Academic Press, p.
224 171–190.
225 Tappa, M. J., Coleman, D.S., Mills, R.D., and Samperton, K.M., 2011, The plutonic record of a
226 silicic ignimbrite from the Latir volcanic field, New Mexico: Geochem. Geophys. Geosyst.,
227 Q10011, doi: 10.1029/2011GC003700.
228 Vaasjoki, M., Rämö, O.T., and Sakko, M., 1991, New U-Pb ages from the Wiborg rapakivi area:
229 constraints on the temporal evolution of the rapakivi granite-anorthosite-diabase dyke
230 association of southeastern Finland: Precambrian Res., v. 51, p. 227-243.
231 Wagner, T.P., Donnelly-Nolan, J.M., and Grove, T.L., 1995, Evidence of hydrous differentiation
232 and crystal accumulation in the low-MgO, high-Al2O3 Lake Basalt from Medicine Lake
233 volcano, California: Contributions to Mineralogy and Petrology, v. 121, p. 201–216,
234 doi:10.1007/s004100050099.

235 Walker Jr., B.A., Miller, C.F., Lowery Claiborne, L., Wooden, J.L., and Miller, J.S., 2007,
236 Geology and geochronology of the Spirit Mountain batholith, southern Nevada: Implications
237 for timescales and physical processes of batholith construction: J. Volcanol. Geotherm. Res.
238 V. 167, p. 239–262.
239 Whittington, A.G., Hofmeister, A.M., and Nabelek, P.I., 2009, Temperature-dependent thermal
240 diffusivity of the Earth's crust and implications for magmatism: Nature, v. 458, p. 319–321,
241 doi:10.1038/nature07818.

Figure DR1
Click here to download high resolution image